MOLECULAR AND CELLULAR BIOLOGY, June 2006, p. 4257–4267 Vol. 26, No. 11
0270-7306/06/$08.00+0 doi:10.1128/MCB.02055-05

Deletion of SERP1/RAMP4, a Component of the Endoplasmic Reticulum (ER) Translocation Sites, Leads to ER Stress

Osamu Hori,[1]* Mayuki Miyazaki,[2] Takashi Tamatani,[1] Kentaro Ozawa,[1] Katsura Takano,[3] Masaru Okabe,[4] Masahito Ikawa,[4] Enno Hartmann,[5] Petra Mai,[5] David M. Stern,[6] Yasuko Kitao,[1] and Satoshi Ogawa[1]

Department of Neuroanatomy, Kanazawa University Graduate School of Medical Science, Kanazawa City, Ishikawa, Japan[1]; Dainippon Pharmaceutical Co., Ltd., Osaka, Japan[2]; Laboratory of Molecular Pharmacology, Kanazawa University Graduate School of Natural Science and Technology, Kanazawa City, Ishikawa, Japan[3]; Genomic Information Service Center, Osaka University, Osaka, Japan[4]; CSCM, Institut für Biologie, Universität Lübeck, Lübeck, Germany[5]; and Dean's Office, University of Cincinnati College of Medicine, Cincinnati, Ohio[6]

Received 22 October 2005/Returned for modification 8 December 2005/Accepted 17 March 2006

Stress-associated endoplasmic reticulum (ER) protein 1 (SERP1), also known as ribosome-associated membrane protein 4 (RAMP4), is a Sec61-associated polypeptide that is induced by ER stress. SERP1$^{-/-}$ mice, made by targeted gene disruption, demonstrated growth retardation, increased mortality, and impaired glucose tolerance. Consistent with high levels of SERP1 expression in pancreas, pancreatic islets from SERP1$^{-/-}$ mice failed to rapidly synthesize proinsulin in response to a glucose load. In addition, reduced size and enhanced ER stress were observed in the anterior pituitary of SERP1$^{-/-}$ mice, and growth hormone production was slowed in SERP1$^{-/-}$ pituitary after insulin stimulation. Experiments using pancreatic microsomes revealed aberrant association of ribosomes and the Sec61 complex and enhanced ER stress in SERP1$^{-/-}$ pancreas. In basal conditions, the Sec61 complex in SERP1$^{-/-}$ microsomes was more cofractionated with ribosomes, compared with SERP1$^{+/+}$ counterparts, in high-salt conditions. In contrast, after glucose stimulation, the complex showed less cofractionation at an early phase (45 min) but more at a later phase (120 min). Although intracellular insulin/proinsulin levels were not significantly changed in both genotypes, these results suggest that subtle changes in translocation efficiency play an important role in the regulation of ER stress and rapid polypeptide synthesis.

Secretory proteins undergo posttranslational processing, including correct folding and oligomerization, in the endoplasmic reticulum (ER). In order to effectively produce and secrete mature proteins, cellular mechanisms for monitoring the ER environment are essential. In mammalian cells, at least three different mechanisms contribute to this surveillance system: regulated induction of transcription, attenuation of translation, and degradation (11). Exposure of cells to conditions promoting accumulation of unfolded proteins in the ER (ER stress) induces molecular chaperones, folding catalysts, and subunits of the translocation machinery (Sec61 complex), a process known as the unfolded protein response. Attenuation of protein synthesis in response to ER stress provides another point of regulation, in this case serving to reduce the load of proteins entering the ER. The latter pathway requires activation of the ER-resident membrane protein PERK and phosphorylation of eukaryotic translation initiation factor 2α (eIF2α) (5).

SERP1 (stress-associated ER protein 1) was identified because of its induction in response to hypoxia or ER stress (20) and found to be identical to RAMP4 (ribosome-associate membrane protein 4). The latter was originally recognized because it was copurified with the Sec61 complex (3, 19) and then found to be a genuine and evolutionarily conserved part of the ER translocon. SERP1/RAMP4 controls glycosylation of major histocompatibility complex class II-associated invariant chains by a translocational pausing mechanism (16), and its overexpression stabilizes newly synthesized membrane proteins under ER stress by associating with the Sec61 complex (20). YSY6, the yeast homolog of SERP1, suppresses the defect in protein export of particular mutant alleles of *secY* in *Escherichia coli* (14). Although these observations suggest that SERP1 is somehow involved in the biosynthesis/processing of secretory proteins, the precise role of SERP1 has not been clarified yet.

We have developed SERP1 knockout mice using a homologous recombination technique and report here that SERP1$^{-/-}$ mice demonstrated postnatal growth retardation, increased mortality, and impaired glucose tolerance. We present evidence that these phenotypes are likely due to the incapability of rapid production of polypeptide hormones by prolonged translational suppression and possible damage of secretory tissues by enhanced ER stress.

MATERIALS AND METHODS

Cell cultures and animal experiments. MIN6 cells were provided by Jun-ichi Miyazaki, Osaka University (10). Cells were cultured in Dulbecco modified Eagle medium (DMEM) (25 mM glucose) with fetal calf serum (15%) and placed in medium with high (25 mM) or low (5.5 mM) glucose when cultures achieved ~70% confluency. Expression of SERP1 or other molecules was analyzed after 24 h. Animal experimental protocols were approved by the Committee on Animal Experimentation of Kanazawa University (Takara-Machi Campus).

* Corresponding author. Mailing address: Department of Neuroanatomy, Kanazawa University, Graduate School of Medical Science, 13-1 Takara-Machi, Kanazawa City, Ishikawa 920-8640, Japan. Phone: 81-76-265-2162. Fax: 81-76-234-4222. E-mail: osamuh@nanat.m.kanazawa-u.ac.jp.

Northern blotting. Hybridization with cDNA fragments of SERP1, Sec61 α and β subunits, or GRP78 was performed as described previously (20). Expression of SERP1 or the Sec61 complex in different tissues was analyzed using human endocrine system MTN Blot, mouse MTN Blot, and mouse MTN Blot II assays (Clontech, Palo Alto, CA).

Western blotting and immunostaining. For MIN6 cells or isolated pancreatic islets, protein extraction was performed in the presence of 1% Triton X-100, 10 mM Tris (pH 7.6), 150 mM NaCl, 1 mM EDTA, 1 mM phenylmethylsulfonyl fluoride (PMSF), 1 μg/ml aprotinin, 1 μg/ml leupeptin, and 1 μg/ml pepstatin. Pancreas, liver, pituitary (anterior and posterior lobes), and cerebral cortex (parietal lobe) were removed from C57BL/6 mice (20 to 25 g) after euthanasia and were homogenized in 1% NP-40, 0.1% sodium dodecyl sulfate (SDS), 0.2% deoxycholate, 10 mM Tris (pH 7.6), 150 mM NaCl, 1 mM EDTA, 1 mM PMSF, 1 μg/ml aprotinin, 1 μg/ml leupeptin, and 1 μg/ml pepstatin. Western blotting was performed with antibodies against SERP1/RAMP4 (3), Sec61α (3), KDEL (StressGen Biotechnologies Corp., Victoria, British Columbia, Canada), Herp (7), P-eIF2α (Cell Signaling Technology, Beverly, MA), eIF2α (Cell Signaling Technology), insulin (Biogenesis, Poole, England, United Kingdom), growth hormone (GH; Biogenesis), corticotropin (ACTH; Chemicon, Temecula, CA), P58 (a gift from M. G. Katze, University of Washington), or β-actin (Sigma, St. Louis, MO). Sites of primary antibody binding were visualized using alkaline phosphatase-conjugated secondary antibodies. For immunostaining, pancreas and other tissues (including pituitary) were removed from C57BL/6 mice (20 to 25 g) after perfusion with paraformaldehyde (4%) and embedded in paraffin, and 5-μm sections were cut. Sections were incubated with anti-insulin antibody or anti-growth hormone antibody (Biogenesis), followed by incubation with fluorescein isothiocyanate- or Cy3-conjugated secondary antibodies.

Development of SERP1 knockout mice. A targeting vector was constructed in pPNT (a gift from Victor L. J. Tybulewicz, MRC National Institute for Medical Research, London, United Kingdom) by replacing exon 1 of the mouse SERP1 gene derived from the 129Sv/J library (Incyte Genomics, St. Louis, MO) with a phosphoglycerate kinase (PGK)-neo cassette (see Fig. 2A). Seven correctly targeted heterozygote embryonic stem cell clones were obtained, and two of those were injected into C57BL/6 blastocysts. Germ line transmission of the SERP1 mutant gene was achieved in both lines. Mice were genotyped by PCR and Southern blotting, and F_1 to F_3 offspring mice were intercrossed (129Sv/J × C57BL/6 background) or backcrossed into the C57BL/6 strain for six generations (C57BL/6 background). In all studies comparing SERP1$^{+/+}$, SERP1$^{+/-}$, and SERP1$^{-/-}$ mice, sex-matched siblings derived from mating SERP1$^{+/-}$ animals were used.

Glucose, insulin, and growth hormone measurements. Blood glucose levels were determined using a portable glucose-measuring device (Dexster-Z; Bayer Medical Co., Tokyo, Japan). Intraperitoneal glucose tolerance tests (i.p.-GTT) and insulin tolerance tests (ITT) were performed by administration of glucose, 2 g/kg of body weight, or insulin, 1 U/kg of body weight, followed by sampling of blood from the tail vein. Insulin and growth hormone levels in culture medium, cell extracts, or plasma were measured by enzyme-linked immunosorbent assay (ELISA) (for insulin, the kit was from Shibayagi Co., Shibukawa, Japan, and for growth hormone, the kit was from Cayman Chemical, Ann Arbor, MI).

Isolation of pancreatic islets and metabolic labeling. Pancreatic islets were isolated from SERP1$^{+/+}$, SERP1$^{+/-}$, or SERP1$^{-/-}$ mice (12 to 16 weeks old) by collagenase digestion, as described previously (4). After incubation in glucose-free RPMI 1640 (Sigma) for 1 h, islets (20 islets/condition) were exposed to high glucose (22 mM), and insulin release was measured as above. Biosynthesis of insulin was evaluated by metabolic labeling as follows. Isolated islets (30 islets/condition) were exposed to high glucose (22 mM) in Met-free DMEM containing dialyzed 10% fetal bovine serum (FBS), and [^{35}S]Met/Cys (200 μCi; Amersham Pharmacia Biotech Inc., Piscataway, NJ) was added for the indicated 30-min periods prior to harvesting. Islet cells were then lysed in 1% Triton X-100, 10 mM Tris, pH 7.6, 150 mM NaCl, 1 mM EDTA, 1 mM PMSF, 1 μg/ml aprotinin, 1 μg/ml leupeptin, and 1 μg/ml pepstatin and immunoprecipitated with anti-insulin antibody. Immunoprecipitates were analyzed on 15% Tricine-buffered polyacrylamide gels followed by autoradiography.

Preparation of recombinant adenoviruses and adenovirus-mediated gene expression. A cDNA fragment spanning the entire coding regions of rat SERP1 and the FLAG epitope (20) was inserted into the pAdx1CA cosmid vector. Recombinant adenovirus Adex1CA SERP1 was prepared by homologous recombination using an adenovirus expression vector kit (Takara, Tokyo, Japan). Viral stocks had titers of ~1×10^9 PFU/ml. A control virus, Adex1CA GFP (green fluorescent protein), was a gift from Hiroshi Kiyama (Osaka City University, Osaka, Japan). Infection of islets was performed as described previously (12). Briefly, isolated islets (40 islets/condition) were incubated with Adex1CA SERP1or Adex1CA GFP (1×10^7 to 2×10^7 PFU/ml) in DMEM containing 5% FBS for 2 h at 37°C, after which RPMI 1640 containing 10% FBS was added. After 36 h, expression of GFP and SERP1 or secretion of insulin was analyzed by immunostaining, Western blotting, or ELISA, respectively, as described above.

Isolation of pancreatic microsomes and in vitro translation/translocation assays. Rough microsomes (RM) from SERP1$^{+/+}$ or SERP1$^{-/-}$ mice (15 to 25 g) were prepared as described previously (17). In brief, mouse pancreas was removed either after 15 h of fasting or after 15 h of starvation followed by glucose stimulation, and two or three pancreata were pooled for each experimental condition. Samples were then homogenized with a tissue grinder (30 s) and a Dounce homogenizer (40 strokes) in ice-cold buffer A, containing 250 mM sucrose, 50 mM triethanolamine, 50 mM KOAc, 6 mM $Mg(OAc)_2$, 1 mM EDTA, 1 mM dithiothreitol, and 0.5 mM PMSF. After sequential centrifugation, the pellets were dissolved in buffer B, containing 250 mM sucrose, 50 mM triethanolamine, and 1 mM dithiothreitol. In vitro translation/translocation analysis was performed using the rabbit reticulocyte lysate system (Promega Corporation, Madison, WI). After the standard reaction using [^{35}S]Met/Cys (200 μCi; Amersham Pharmacia Biotech Inc.) for 30 min at 30°C, half of the samples (12.5 μl) were precipitated with 20% trichloroacetic acid. The pellets were washed with acetone and dissolved in SDS sample buffer. The newly synthesized proteins (β-lactamase and luciferase) were resolved by SDS-polyacrylamide gel electrophoresis (10% gel) followed by autoradiography. In vitro translation/translocation analysis of growth hormone, prolactin, and insulin was also performed in the presence of ribosome-free membranes (K-RM) for both genotypes (2). One equivalent was determined as described previously (17).

Fractionation of RM by iodixanol gradient centrifugation. Fractionation of RM was performed essentially as described previously (2), with some modification. In brief, RM were dissolved at 0.5 eq/μl either in low-salt buffer (100 mM KOAc), high-salt buffer (600 mM KOAc), or high-salt buffer (600 mM KOAc) with 1 mM puromycin, containing 0.04% deoxycholate, 50 mM HEPES (pH 7.5), 6 mM $Mg(OAc)_2$, 0.25 M sucrose, and 0.5 mM PMSF. The samples were incubated at room temperature for 20 min and then layered onto 20 to 30% iodixanol (Opti-prep; Axis-Shield PoC AS, Oslo, Norway) gradients in the same buffers as those for dissolving RM. After centrifugation in a TLA 100.4 rotor at 50,000 rpm for 140 min, fractions were subjected to Western blotting with indicated antibodies.

Laser densitometric analysis and measurement of pancreatic islets and pituitary. Laser densitometric analysis was performed to semiquantitate results of Western and Northern blotting as described previously (7). The sizes of pancreatic islets, pituitary anterior lobes, and intermediate/posterior lobes were measured using Adobe Photoshop 6.0 (Adobe Systems Inc., San Jose, CA).

RESULTS

Expression of SERP1 in secretory tissue. In order to identify a model system for the analysis of SERP1 function, its expression was determined in different human and mouse organs (Fig. 1AI and AII; also data not shown). SERP1 transcripts, together with those of the Sec61 complex, were expressed at high levels in secretory organs such as pancreas, prostate, and salivary gland (Fig. 1AI and AII) and, to a slightly lesser extent, in liver (data not shown). While mouse and rat organs had a prominent transcript of 2.3 kb as described previously for rat tissues (Fig. 1AII) (20), human cells contained an additional SERP1 transcript of approximately 0.9 kb. PCR and Northern blot analysis using different sets of primers/probes suggested that both transcripts were derived from the human SERP1 gene but that they had different poly(A) attachment sites (data not shown).

As expressions of the Sec61 complex and other translocon members were reportedly upregulated in MIN6 cells, a mouse insulinoma cell line, after exposure to high glucose (18), the levels of SERP1 expression in these cells were compared in the presence of low (5.5 mM) and high (25 mM) glucose. Both SERP1 transcripts and antigens increased under high-glucose conditions to a similar extent as the Sec61 complex (~2.2-fold increase at RNA level [Fig. 1BI] and ~2.4-fold at antigen level

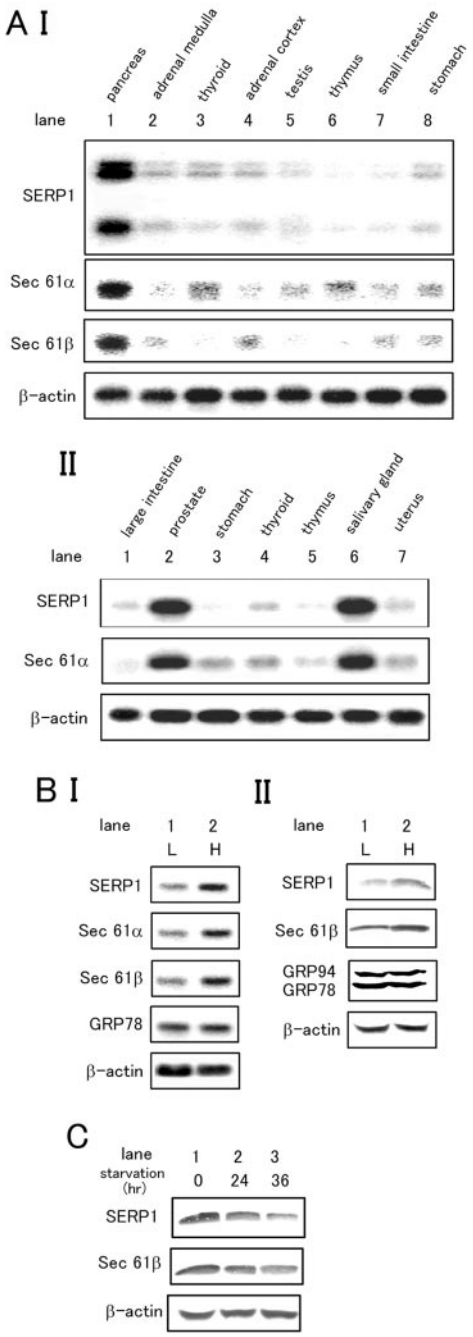

FIG. 1. Expression of SERP1 in secretory tissue. A. Expression of SERP1 and Sec61 complex in human and mouse secretory tissue. Human endocrine system MTN Blot (I) or mouse MTN Blot II (II) was hybridized with indicated ^{32}P-labeled cDNA probes. B. Expression of SERP1 and the complex in MIN6 cells. I. MIN6 cells (10^7 cells/condition) were incubated in medium containing high (H; 25 mM) or low (L; 5.5 mM) glucose for 24 h, and total RNA (10 μg/lane) was used for Northern blotting. II. MIN6 cells (5×10^6 cells/condition) were incubated as described above, and cell extracts were subjected to Western blotting using indicated antibodies. C. Expression of SERP1 and the Sec61 complex in pancreas. Protein extracts of pancreas from C57BL/6 mice after starvation for indicated times were subjected to Western blotting as described above.

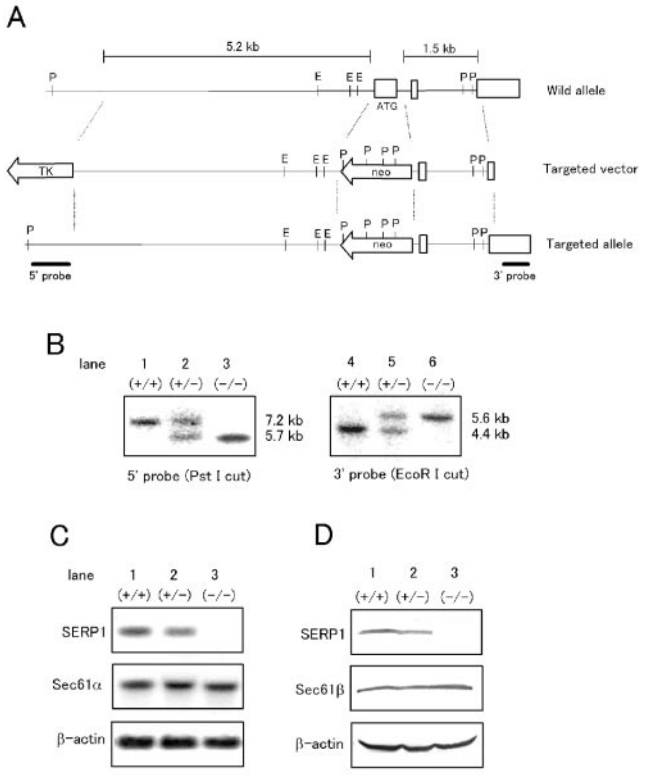

FIG. 2. Generation of SERP1$^{-/-}$ mice. A. Creation of the mutant allele by homologous recombination. The neomycin resistance gene was flanked by 5.2 and 1.5 kb of 5′ and 3′ genomic sequences and replaced exon 1 of the mouse SERP1 gene, including the start codon (ATG). TK, PGK-thymidine kinase (TK) cassette; neo, PGK-neomycin resistance gene (neo) cassette; E, EcoRI; P, PstI. B. Southern blotting of mouse tail DNA in a litter born to two heterozygotes (SERP$^{+/-}$). Purified DNA was digested with PstI (lanes 1 to 3) or EcoRI (lanes 4 to 6) and hybridized with 5′ or 3′ probes indicated in panel A. The mutated allele (5.7 and 5.6 kb) could be distinguished from the wild-type allele (7.2 and 4.4 kb) in each case. C and D. Expression of SERP1 transcripts (C) and antigens (D) in SERP1$^{+/+}$, SERP1$^{+/-}$, and SERP1$^{-/-}$ mice at 3 weeks after birth. Total liver RNA (20 μg) was hybridized with ^{32}P-labeled cDNA probes as described in the text (C). Protein extracts (40 μg) from pancreas were subjected to Western blotting with indicated antibodies.

[Fig. 1BII]). Accordingly, the levels of expression of SERP1 and Sec61 complex antigens in the whole pancreas decreased by starvation in vivo (Fig. 1C).

Generation of SERP1 knockout mice and effects of the SERP1 gene deletion on development. To study the function of SERP1 in vivo, we created mice lacking SERP1. Targeted disruption of the SERP1 gene was performed (Materials and Methods) (Fig. 2A). Homologous recombinants of the SERP1 gene were correctly transmitted (Fig. 2B), and expression of SERP1 was not observed in SERP1 knockout mice both at the level of transcription (Fig. 2C) and at the level of translation (Fig. 2D).

SERP1$^{-/-}$ mice were born almost at the expected Mendelian ratio, and there was no apparent phenotype observed except for a slight reduction in body weight compared with SERP1$^{+/+}$ and SERP1$^{+/-}$ mice (0.9 ± 0.1 g for SERP1$^{-/-}$ and 1.0 ± 0.1 g for other genotypes). However, by 3 weeks of

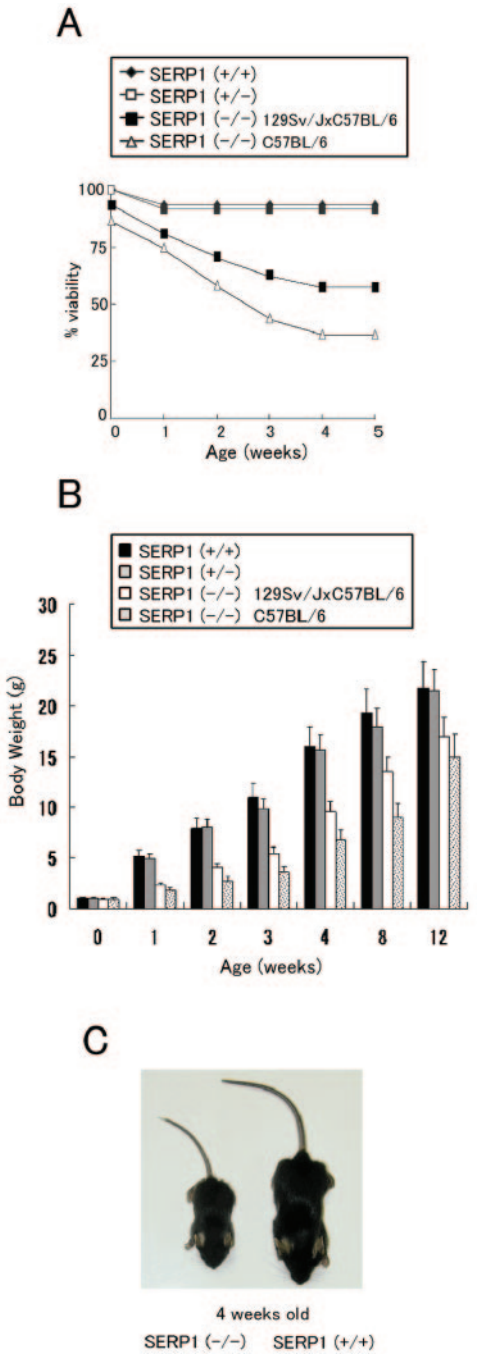

FIG. 3. Postnatal growth retardation in SERP1$^{-/-}$ mice. A. Survival of neonatal SERP1$^{+/+}$, SERP1$^{+/-}$, and SERP1$^{-/-}$ mice. The number of mice at birth was designated as 100 in each group. SERP1$^{-/-}$ mice in a C57BL/6 background have lower viability than SERP1$^{-/-}$ mice in a 129Sv/J × C57BL/6 background. B. Weight gain in neonatal genetically manipulated SERP1 mice of the indicated genotype. C. Representative photograph of SERP1$^{-/-}$ versus SERP1$^{+/+}$ littermate siblings in the 129Vs/J × C57BL/6 background.

age, SERP1$^{-/-}$ mice displayed increased mortality (Fig. 3A) and growth retardation (Fig. 3B). Approximately 60% and 35% of SERP1$^{-/-}$ mice in a mixed 129Sv/J × C57BL/6 (n = 16) and C57BL/6 (n = 12) background, respectively, grew to adulthood (Fig. 3A). Body weights of SERP1$^{-/-}$ mice were reduced to 60% ± 12% of those of SERP1$^{+/+}$ mice in the 129Sv/J × C57BL/6 and to 44% ± 13% of those of SERP1$^{+/+}$ mice in the C57BL/6 mice at 4 weeks after birth. If the body weight of a SERP1$^{-/-}$ mouse was less than 40% of that of a SERP1$^{+/+}$ mouse of the same age, or if weight gain stopped for several days, these animals would usually die. Autopsies of nonsurviving SERP1$^{-/-}$ mice revealed amounts of milk in the gut comparable to those of other mice. Blood glucose levels and liver glycogen contents of low-weight SERP$^{-/-}$ animals were not significantly different from those of other genotypes during the period from 1 to 4 weeks of age. These data indicate that the high mortality of SERP$^{-/-}$ mice was not likely due to reduced nursing or impaired intestinal absorption.

Once SERP1$^{-/-}$ mice survived to the age of 4 weeks, their growth and body weight steadily increased. By 12 weeks of age, body weights of SERP1$^{-/-}$ animals recovered to ~75% of those of SERP1$^{+/+}$ mice in both backgrounds (Fig. 3B).

Effects of the SERP1 gene deletion on glucose homeostasis and insulin biosynthesis. High levels of SERP1 expression in pancreas and in MIN6 cells (Fig. 1) led us to investigate the role of SERP1 in glucose homeostasis and insulin biosynthesis/secretion. i.p.-GTT were performed using mice between 10 and 20 weeks of age to minimize the effect of growth retardation in SERP1$^{-/-}$ mice. Both male and female SERP1$^{-/-}$ mice revealed impaired glucose tolerance (Fig. 4AI and AII). Increased blood glucose levels in SERP1$^{-/-}$ mice were most prominent between 30 min and 60 min after glucose infusion. In the later phase (120 min after glucose injection) of i.p.-GTT, glucose levels in SERP1$^{-/-}$ mice were close to that observed in wild-type controls. In contrast, ITT revealed no significant difference in blood glucose levels between SERP1$^{+/+}$ and SERP1$^{-/-}$ mice after insulin administration (data not shown), suggesting that impaired glucose tolerance in SERP1$^{-/-}$ animals was not due to insulin resistance in peripheral tissue. Histological analysis of pancreatic tissue demonstrated islets of comparable size (Fig. 4B) and immunoreactivity with anti-insulin antibody (data not shown) when SERP1$^{-/-}$ mice were compared with wild-type controls.

To further analyze the effect of SERP1 on insulin biosynthesis/secretion, pancreatic islets were isolated from mice and stimulated by exposure to media with high glucose (22 mM; Fig. 4C). There was only a slight difference in insulin secretion at 15 min after stimulation when islets from the different genotypes were compared (SERP1$^{+/+}$, SERP1$^{+/-}$, and SERP1$^{-/-}$). However, by 30 to 60 min, insulin secretion continued to increase in islets from wild-type controls but not in islets from SERP1$^{-/-}$ mice. It was not until the 60- to 120-min time period that insulin secretion in islets from SERP1$^{-/-}$ mice began to increase again. By 120 min, comparable levels of insulin were present in the supernatants of islets from each genotype.

Metabolic labeling of isolated islets followed by immunoprecipitation with anti-insulin antibody was performed to measure proinsulin/insulin biosynthesis/processing directly after glucose stimulation. In islets from SERP1$^{+/+}$ mice, proinsulin biosynthesis started and reached a peak at 30 to 60 min after glucose stimulation (Fig. 4D, lane 2). Thereafter, it gradually decreased (Fig. 4D, lanes 3 and 4). In contrast, islets from SERP1$^{-/-}$ mice showed a delay in proinsulin biosynthesis that

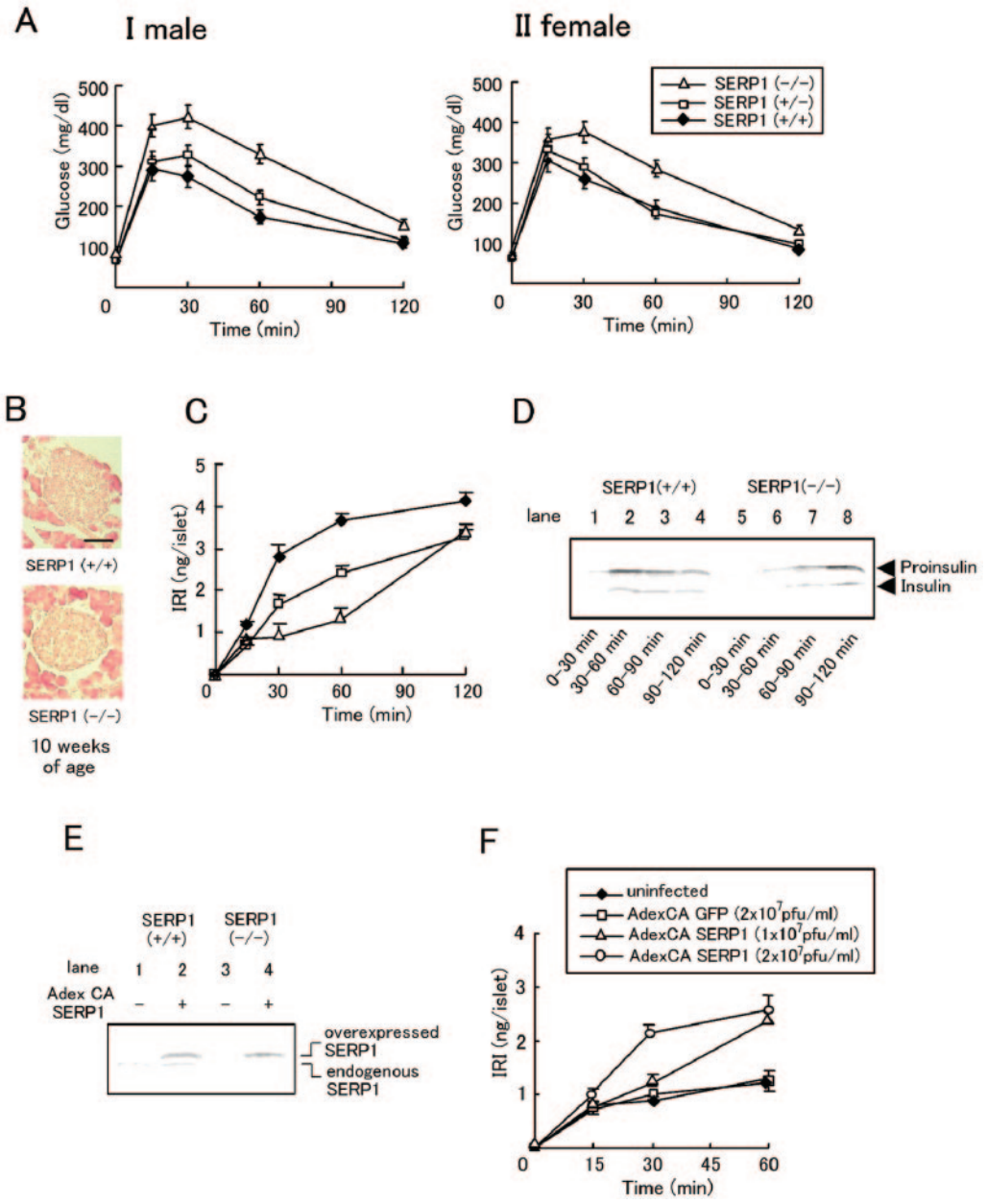

FIG. 4. Impaired glucose tolerance and delayed biosynthesis of insulin in SERP1$^{-/-}$ mice. A. i.p.-GTT were performed on SERP1$^{+/+}$, SERP1$^{+/-}$, and SERP1$^{-/-}$ mice at 10 weeks. Values shown are means ± standard deviations (n = 10 in panel I and n = 6 in panel II). B. Hematoxylin-and-eosin-stained SERP1$^{-/-}$ and SERP1$^{+/+}$ pancreas (10 weeks of age). Bar, 50 μm. C. Insulin release from pancreatic islets isolated from SERP1 mice of the indicated genotype. Islets were incubated in medium containing 22 mM glucose for the indicated times. Insulin levels in the medium were measured by ELISA. Values shown are means ± standard deviations (n = 4). D. Insulin biosynthesis in SERP1$^{+/+}$ (lanes 1 to 4) and SERP1$^{-/-}$ (lanes 5 to 8) islets. Islets were stimulated with high glucose (22 mM) and subjected to metabolic labeling with [^{35}S]Met/Cys for 30 min prior to harvesting. Cell extracts were immunoprecipitated with anti-insulin antibody. E. Adenovirus-mediated transfer of SERP1 cDNA. SERP1$^{+/+}$ and SERP1$^{-/-}$ islets were infected with AdexCA SERP1 (2×10^7 PFU/nl) (lanes 2 and 4) or cultured in the medium alone (lanes 1 and 3), and cell extracts were subjected to Western blotting with anti-SERP1 antibody. F. Rescue experiments with SERP1 cDNA. SERP1$^{-/-}$ islets were infected with AdexCA SERP1 (1×10^7 to 2×10^7 PFU/nl) or AdexCA GFP (2×10^7 PFU/nl) or cultured in medium alone. Insulin release in response to glucose stimulation (22 mM) was monitored by ELISA. Values shown are means ± standard deviations (n = 3).

peaked at 90 to 120 min after glucose stimulation (Fig. 4D, lane 8). The ratio of proinsulin to insulin was not significantly changed in islets from SERP1$^{-/-}$ and wild-type control mice, suggesting that the SERP1 gene deletion affects the biosynthesis of proinsulin but not the conversion of proinsulin to insulin.

To confirm that delayed proinsulin biosynthesis in SERP1$^{-/-}$ islets was due to deletion of the SERP1 gene, rescue experiments were performed using adenovirus-mediated transfer of the SERP1 cDNA as described previously (12). When isolated islets were infected with AdexCA SERP1 (2×10^7 PFU/ml),

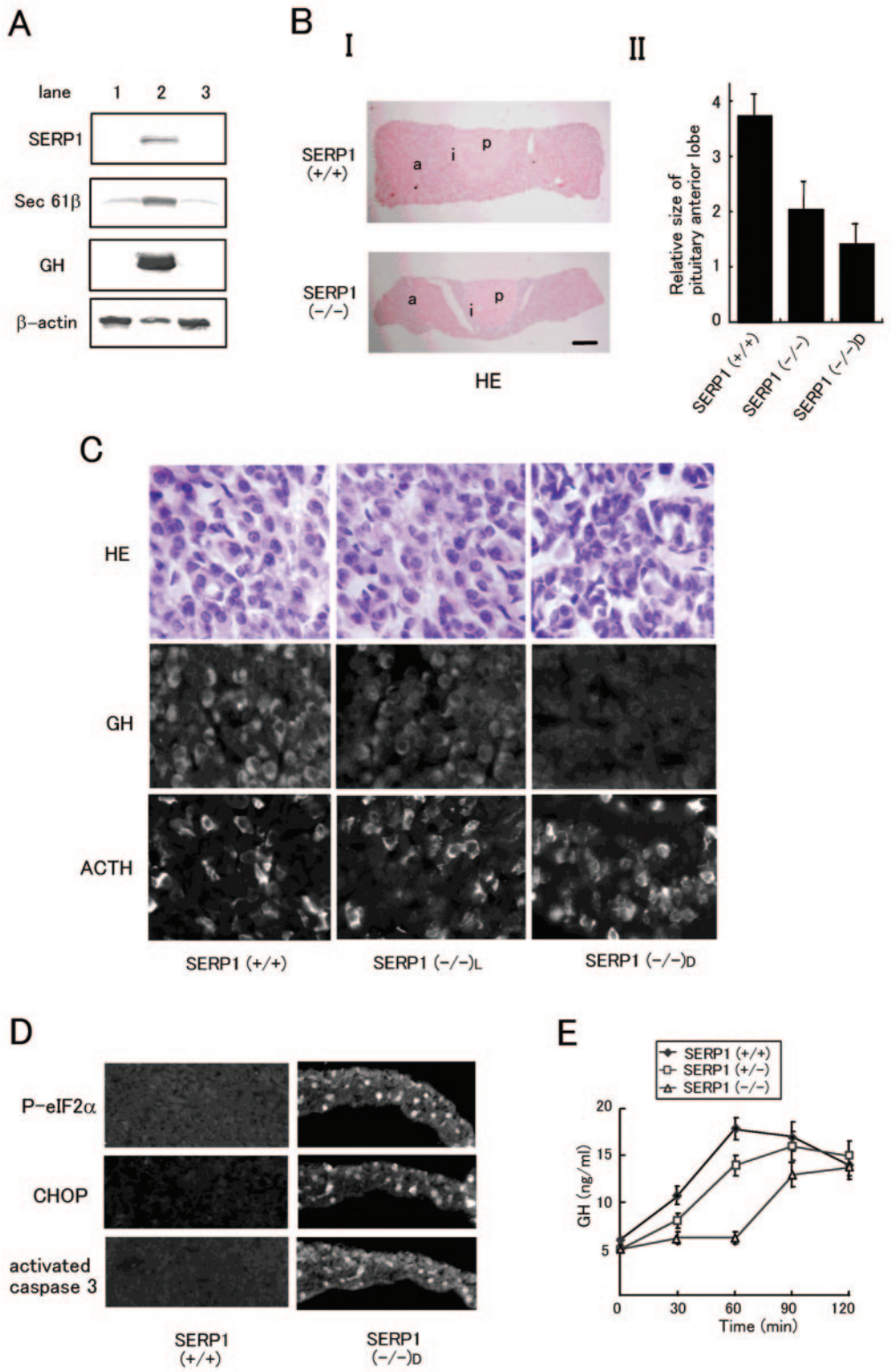

FIG. 5. Reduced size and enhanced ER stress in the SERP1$^{-/-}$ anterior pituitary. A. Expression of SERP1, Sec61β, and GH in the pituitary. Protein extracts (40 μg) from cerebral cortex (lane 1) or pituitary anterior (lane 2) or posterior (lane 3) lobe of C57BL/6 mice (8 weeks) were subjected to Western blotting with indicated antibodies. B. The size of pituitary anterior lobe. I. Pituitary from mice of the indicated genotype (4 to 8 weeks old, coronal section) was stained with hematoxylin and eosin (n = 4), and representative micrographs are shown. Bar, 200 μm. II. Relative size of pituitary anterior lobe in SERP1$^{+/+}$, total SERP1$^{-/-}$ (SERP1$^{-/-}$), and dying SERP1$^{-/-}$ (SERP1$^{-/-}$*D*) mice. Area occupied by the anterior (a) lobe was divided by the combined area of posterior (p) and intermediate (i) (area of the p + i lobes was designated as 1). Values shown are means ± standard deviations (n = 4). C. Expressions of GH and ACTH in the anterior pituitary. Pituitary from SERP1$^{+/+}$, living

overexpression of SERP1 antigen was detected by Western blotting as an immunoreactive band just above endogenous SERP1, probably due to the presence of the FLAG epitope (Fig. 4E). In our system, approximately 80% of cells were infected with AdexCA GFP or AdexCA SERP1 at a virus titer of 2×10^7 PFU/ml, based on morphological studies. Adenovirus-infected islets were stimulated in the presence of glucose (22 mM), and insulin secretion was monitored. Insulin secretion was enhanced in a dose-dependent manner in SERP1$^{-/-}$ islets subjected to SERP1 gene transfer 30 to 60 min after glucose challenge (Fig. 4F). Overexpression of GFP, in contrast, was without effect on insulin secretion (Fig. 4F).

Effects of SERP1 gene deletion on the pituitary. Temporal growth retardation in SERP1$^{-/-}$ mice during the postnatal period suggested the possibility that SERP1 might also play an important role in the biosynthesis/secretion of hormones associated with neonatal development. Western blotting of protein extracts from wild-type mouse brain (cerebral cortex) and pituitary anterior and posterior lobes disclosed that both SERP1 and the Sec61 complex (Sec61β) were highly expressed in the anterior pituitary (Fig. 5A). Further analysis using young mice (3 to 8 weeks of age) from each genotype in a 129Sv/J × C57BL/6 background revealed that the anterior pituitary was reduced in size in SERP1$^{-/-}$ mice, compared with wild-type controls, while the intermediate and posterior ones were not affected (Fig. 5BI). The area of the anterior lobe (a) is increased 3.6-fold over that of the posterior (p) and intermediate (i) lobes in SERP1$^{+/+}$ mice and increased 2.0-fold in SERP1$^{-/-}$ mice [Fig. 5BII, SERP1(+/+) and SERP1(−/−), respectively]. To analyze possible mechanisms underlying the higher mortality in SERP1$^{-/-}$ mice, mutant animals whose body weights were less than 40% of those of SERP1$^{+/+}$ mice were grouped and designated SERP1$^{-/-}$*D* mice (dying mice). The relative size of the pituitary anterior lobe in SERP1$^{-/-}$*D* mice was further reduced [Fig. 5BII, SERP1$(-/-)_D$; 1.5-fold increase of posterior (p) and intermediate (i) lobes]. Morphological analysis revealed that cells present in the anterior pituitary of living SERP1$^{-/-}$ mice (SERP1$^{-/-}$*L*) had the same approximate size as those in the other genotypes, while those in the SERP1$^{-/-}$*D* mice had a smaller size and a smaller area of cytosol (Fig. 5C). Immunohistochemical analysis showed diminished expression of GH, but not of ACTH, in SERP1$^{-/-}$ pituitary (Fig. 5C). Furthermore, expression/activation of molecules associated with ER stress/ER stress-induced cell death was clearly observed in SERP1$^{-/-}$*D* mice (Fig. 5D).

The overall size/mass of other endocrine tissues or target organs, such as adrenal gland, thyroid, skeletal muscle, and bone, was also relatively reduced in SERP1$^{-/-}$ mice during the neonatal period by up to 60 to 70% compared with SERP1$^{+/+}$ mice. Such widespread changes, however, may be due to nonspecific effects of general growth retardation in SERP1$^{-/-}$ mice.

To analyze the effect of the SERP1 gene deletion on GH biosynthesis and/or secretion, ITT were performed, and blood GH levels were monitored in adult mice (8 weeks old) of each of the genotypes in the 129Sv/J × C57BL/6 background (Fig. 5E). In SERP1$^{+/+}$ mice, blood GH increased in response to hypoglycemia, reaching peak levels by 60 min after insulin infusion (18 ± 2.1 ng/ml). In contrast, there was no increase of GH levels in SERP1$^{-/-}$ mice until the 60-min time point (6 ± 0.5 ng/ml). At 90 min, GH levels in wild-type mice began a gradual decline, while GH levels continued to increase in SERP1$^{-/-}$ mice. After 120 min, each group had similar growth hormone levels (13 to 15 ng/ml).

Effects of the SERP1 gene deletion on the protein translocation and translocation apparatus. To dissect the mechanisms through which SERP1 contributes to rapid biosynthesis of polypeptide hormones in response to stimuli, pancreatic RM were isolated from SERP1$^{+/+}$ and SERP1$^{-/-}$ mice after overnight starvation as described previously (17). Western blot analysis revealed that expression of ER stress-related proteins, such as GRP94, GRP78, or Herp, was enhanced in SERP1$^{-/-}$ RM, compared with wild-type ones (1.5- to 2-fold increase in SERP1$^{-/-}$ RM). Herp is a novel sensitive marker of ER stress that is rapidly degraded at the protein level (7). Phosphorylation of eIF2α, which is responsible for the suppression of protein synthesis in response to ER stress, was also observed to a greater extent in SERP1$^{-/-}$ mice (1.5-fold increase in SERP1$^{-/-}$ RM). In contrast, the amount of membrane-associated ribosomal protein S6 (RPS6) was slightly reduced in SERP1$^{-/-}$ RM (0.7-fold in SERP1$^{-/-}$ RM), and expression of the Sec61 complex (α and β subunits) was similar in both SERP1$^{+/+}$ and SERP1$^{-/-}$ RM (Fig. 6AI and AII). Intracellular insulin/proinsulin levels, determined by ELISA and immunohistochemistry, were not significantly different in the two genotypes (data not shown).

To analyze the effect of SERP1 on protein translocation, an in vitro translation/translocation assay was performed using rabbit reticulocyte lysates. As expected, translation of mRNA of the secretory protein β-lactamase in the absence of canine RM resulted in the synthesis of a precursor containing the signal sequence, while the same reaction performed in the presence of canine RM led to the production of the mature form (Fig. 6B, lanes 1 and 2). Coincubation of β-lactamase mRNA with SERP1$^{+/+}$ or SERP1$^{-/-}$ RM (0.5 to 2 eq) also synthesized processed protein in a dose-dependent manner (Fig. 6B, lanes 3 to 10). However, the yields of both mature and precursor protein were remarkably reduced in the presence of SERP1$^{-/-}$ RM. Coincubation of luciferase (a cytosol protein) mRNA (0.5 to 2 eq) with RM also resulted in reduced protein synthesis (translation) in the presence of SERP1$^{-/-}$ RM (Fig. 6B, lower panel), suggesting that general protein synthesis was inhibited to a greater extent by SERP1$^{-/-}$ RM. A similar trend was obtained when growth hormone (data not shown), prolactin,

SERP1$^{-/-}$ (SERP1$^{-/-}$*L*), and dying SERP1$^{-/-}$ (SERP1$^{-/-}$*D*) mice was stained with hematoxylin and eosin (HE) or immunostained with anti-GH and anti-ACTH antibody. D. Expression/activation of molecules associated with ER stress-induced cell death. Pituitary from SERP1$^{+/+}$ or dying SERP1$^{-/-}$ (SERP1$^{-/-}$*D*) mice was immunostained with the indicated antibodies. E. GH biosynthesis/secretion in SERP1 mice of the indicated genotype (8 weeks of age) after insulin stimulation. ITT were performed as described in Fig. 4, and blood GH levels were measured by ELISA at the indicated times. Values shown are means ± standard deviations ($n = 4$).

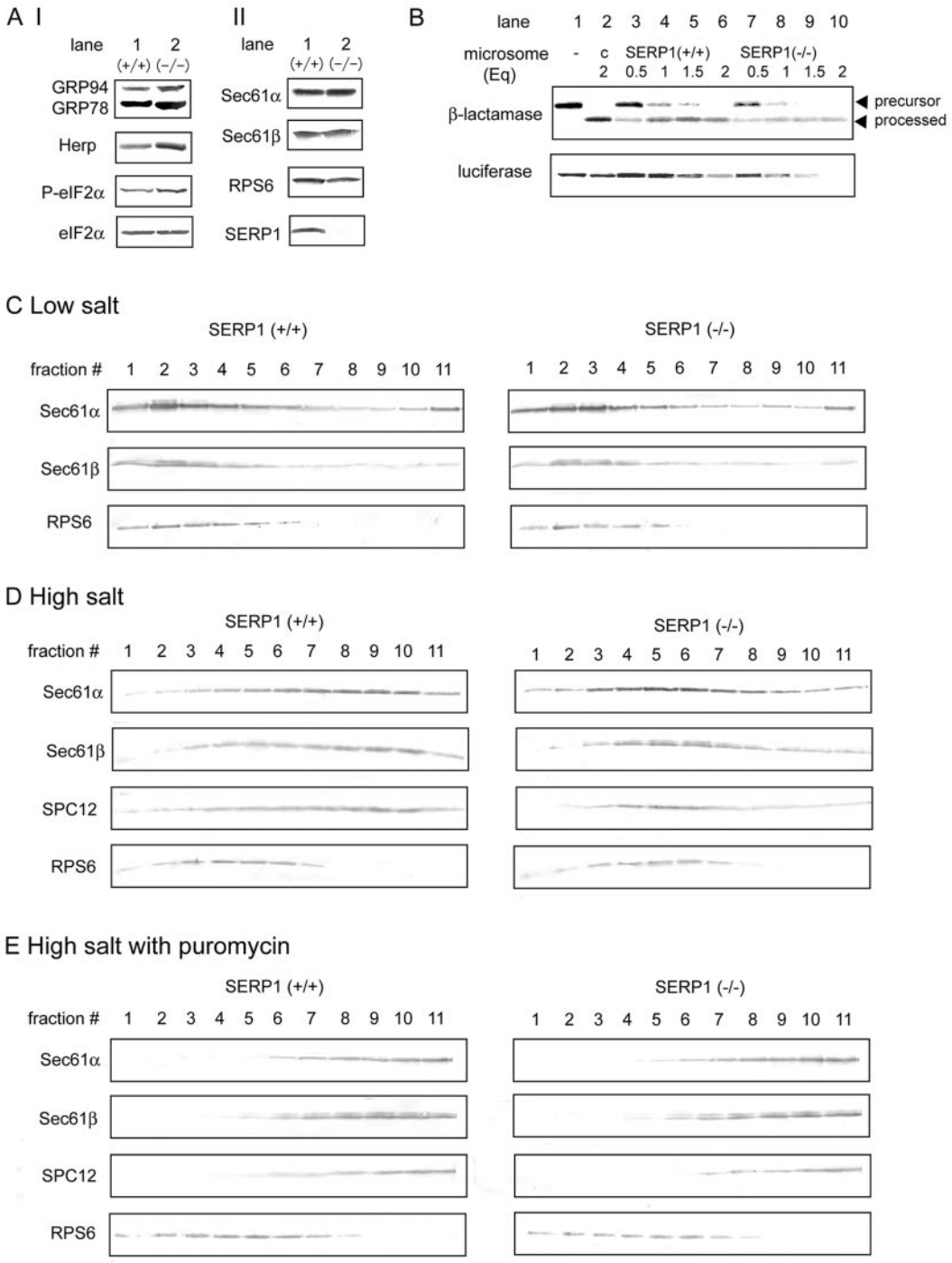

FIG. 6. Characterization of pancreatic RM under basal conditions. A. Expression of ER stress-related molecules and Sec61-associated molecules. RM were isolated from SERP1$^{+/+}$ and SERP1$^{-/-}$ pancreas after 15 h of starvation, as described in the text, and subjected to Western blotting (10 eq/sample) using the indicated antibodies. A typical result of three experiments with independently prepared RM is shown. B. In vitro translation/translocation assay. β-Lactamase (0.1 μg) or luciferase mRNA (0.1 μg) was translated in rabbit reticulocyte lysates in the absence of microsomes (lane 1) or in the presence of canine pancreatic microsomes (2 eq; lane 2), SERP1$^{+/+}$ pancreatic microsomes (0.5 to 2 eq; lanes 3 to 6), or SERP1$^{-/-}$ pancreatic microsomes (0.5 to 2 eq; lanes 7 to 10) for 30 min at 30°C. A typical result of three experiments with independently prepared RM is shown. C to E. Fractionation of RM. RM samples were fractionated using an iodixanol gradient (20 to 30%) in low-salt (C), high-salt (D), and high-salt with puromycin (E) conditions as described in the text and subjected to Western blotting with the indicated antibodies. A typical result of three experiments with independently prepared RM is shown.

or insulin (data not shown) mRNA was used as substrate in ribosome-depleted microsomes (K-RM) from SERP1$^{+/+}$ and SERP1$^{-/-}$ mice.

Fractionation analysis was then performed to compare the status of protein translocation in SERP1$^{+/+}$ and SERP1$^{-/-}$ RM in vivo (2). RM were incubated in low-salt buffer (100 mM KCl) (Fig. 6C), high-salt buffer (600 mM KCl) (Fig. 6D), or high-salt buffer with puromycin (600 mM KCl and 1 mM puromycin) (Fig. 6E) and then fractionated using an iodixanol gradient (20 to 30%). In low-salt conditions, the majority of Sec61 complex cofractionated with the ribosomal protein RPS6, in both SERP1$^{+/+}$ and SERP1$^{-/-}$ RM. However, in high-salt buffer, where translocating polypeptide-free Sec61 was separated from ribosomes, the Sec61 complex and signal peptidase complex 12 (SPC12) cofractionated to a greater extent with RPS6 in SERP1$^{-/-}$ RM, compared with SERP1$^{+/+}$ RM (Fig. 6D). Quantitative studies demonstrated that 50% and 51% of Sec61α and -β, respectively, cofractionated with RPS6 in SERP1$^{+/+}$ RM, while 71% and 69% of Sec61α and -β, respectively, cofractionated with RPS6 in SERP1$^{-/-}$ RM under high-salt conditions (Fig. 7DI and DII; time zero). Addition of puromycin under high-salt conditions separated the Sec61 complex from RPS6 in both genotypes (Fig. 6E), confirming the specific association of Sec61complex with polypeptide-translocating ribosomes in high-salt conditions.

To gain further insight into the mechanism of delayed biosynthesis of insulin/proinsulin in SERP1$^{-/-}$ mice, RM were isolated from both genotypes 45 min and 120 min after glucose stimulation. Western blot analysis revealed that expression of Herp was enhanced at both time points in SERP1$^{-/-}$ RM, compared with SERP1$^{+/+}$ RM, although this increase was less evident 120 min after glucose stimulation (Fig. 7AI). In contrast, phosphorylated eIF2α in SERP1$^{-/-}$ RM was enhanced at 45 min after glucose stimulation, though this declined to the baseline levels, comparable to that in SERP1$^{+/+}$ RM, by 120 min (Fig. 7AI). Quantitative analysis of phosphorylated eIF2α (P-eIF2α) confirmed enhanced phosphorylation of eIF2α in SERP1$^{-/-}$ RM up to 60 min after glucose stimulation, compared with observations in SERP1$^{+/+}$ RM (Fig. 7AII). There was also a slight increase of P-eIF2α immunoreactivity under basal conditions (zero point) in SERP1$^{+/+}$ RM as previously reported (22).

Further fractionation analysis of RM in high-salt conditions revealed that the Sec61 complex cofractionated to a lesser extent with RPS6 in SERP1$^{-/-}$ RM, compared with SERP1$^{+/+}$ RM, at 45 min after glucose exposure (Fig. 7B). In contrast, at 120 min after glucose stimulation, the Sec61 complex again (as in the absence of glucose stimulation [Fig. 6D]) cofractionated to a greater extent with RPS6 in SERP1$^{-/-}$ RM (Fig. 7D). Quantitative analysis showed that, at 45 min, 66% and 68% of Sec61α and -β, respectively, cofractionated with RPS6 in SERP1$^{+/+}$ RM, while 48% and 42% of Sec61α and -β, respectively, cofractionated with RPS6 in SERP1$^{-/-}$ RM (Fig. 7DI and DII; 45 min). At 120 min, in contrast, 63% and 58% of Sec61α and -β, respectively, cofractionated with RPS6 in SERP1$^{+/+}$ RM, while 70% and 71% of Sec61α and -β, respectively, cofractionated in SERP1$^{-/-}$ RM (Fig. 7DI and DII; 120 min).

DISCUSSION

In the current study, we first demonstrated that SERP1, together with the Sec61 complex, was highly expressed in both endocrine and exocrine systems, and its expression was upregulated in response to high glucose. Although deletion of the YSY6 gene, the yeast homolog of SERP1, did not show any apparent phenotype in yeast (unpublished observation), impaired glucose tolerance was observed in SERP1$^{-/-}$ mice at 10 weeks of age. SERP1$^{-/-}$ mice displayed impaired glucose tolerance characterized by a delay in the peak blood glucose levels at 30 min and recovery, with restitution of blood glucose to the range observed in wild-type animals, by 120 min (Fig. 4A). Consistent with these observations, pancreatic islets from SERP1$^{-/-}$ mice displayed a prominent delay of insulin secretion/biosynthesis after glucose challenge (Fig. 4C and D). Although the effect of SERP1 expression was associated with proinsulin biosynthesis which occurs at the ER membrane (Fig. 4D) (8, 19), it is also possible that SERP1 contributes to insulin secretion or energy metabolism in islet cells through the biosynthesis of unknown proteins.

SERP1$^{-/-}$ mice also revealed postnatal growth retardation and increased mortality compared with SERP1$^{+/+}$ littermates. Our search for a cause of growth retardation in SERP1$^{-/-}$ mice led to an investigation of the pituitary. High levels of SERP1 expression were observed in the anterior lobe of the pituitary (Fig. 5A), and its size was significantly smaller in SERP1$^{-/-}$ mice than in wild-type controls (Fig. 5BI and BII). Morphological analysis revealed reduced expression of GH and enhanced ER stress in SERP1$^{-/-}$ mice (Fig. 5C and D). These results suggest that growth arrest and cell death due to enhanced ER stress (1, 13) in the anterior pituitary may be one of the major causes of postnatal growth retardation in SERP1$^{-/-}$ mice. Our preliminary results revealed almost intact morphology and expression of the GH-RH protein in SERP1$^{-/-}$ hypothalamus (data not shown). Analogous to the delayed insulin biosynthesis in response to glucose loads, insulin-stimulated GH production was delayed in adult SERP1$^{-/-}$ mice (Fig. 5E).

Experiments using pancreatic microsomes demonstrated enhanced ER stress (Fig. 6A) and suppression of protein translation (Fig. 6B) in SERP1$^{-/-}$ pancreas, while SERP1 itself did not facilitate translocation of polypeptides in vitro (Fig. 6B; data not shown). Fractionation experiments under basal conditions (i.e., no glucose stimulation) with high salt demonstrated that more Sec61 complexes were tightly associated with ribosomes in SERP1$^{-/-}$ RM than in SERP1$^{+/+}$ RM (Fig. 6D), suggesting that SERP1$^{-/-}$ RM retain more translocating polypeptides at translocation sites. However, intracellular insulin/proinsulin levels (data not shown) or proinsulin biosynthesis in vivo (Fig. 4D, lanes 1 and 5) was not significantly changed in both genotypes, and overall synthesis of β-lactamase (Fig. 6B) or other polypeptide hormones (data not shown) in vitro was suppressed in SERP1$^{-/-}$ RM. Taken together, these observations lead to a hypothesis that SERP1 slightly changes the translocation efficiency in vivo but that its defect is compensated for by an enhanced ER stress response in basal conditions.

Once SERP1$^{+/+}$ and SERP1$^{-/-}$ mice received a glucose challenge, however, the effect of enhanced ER stress in

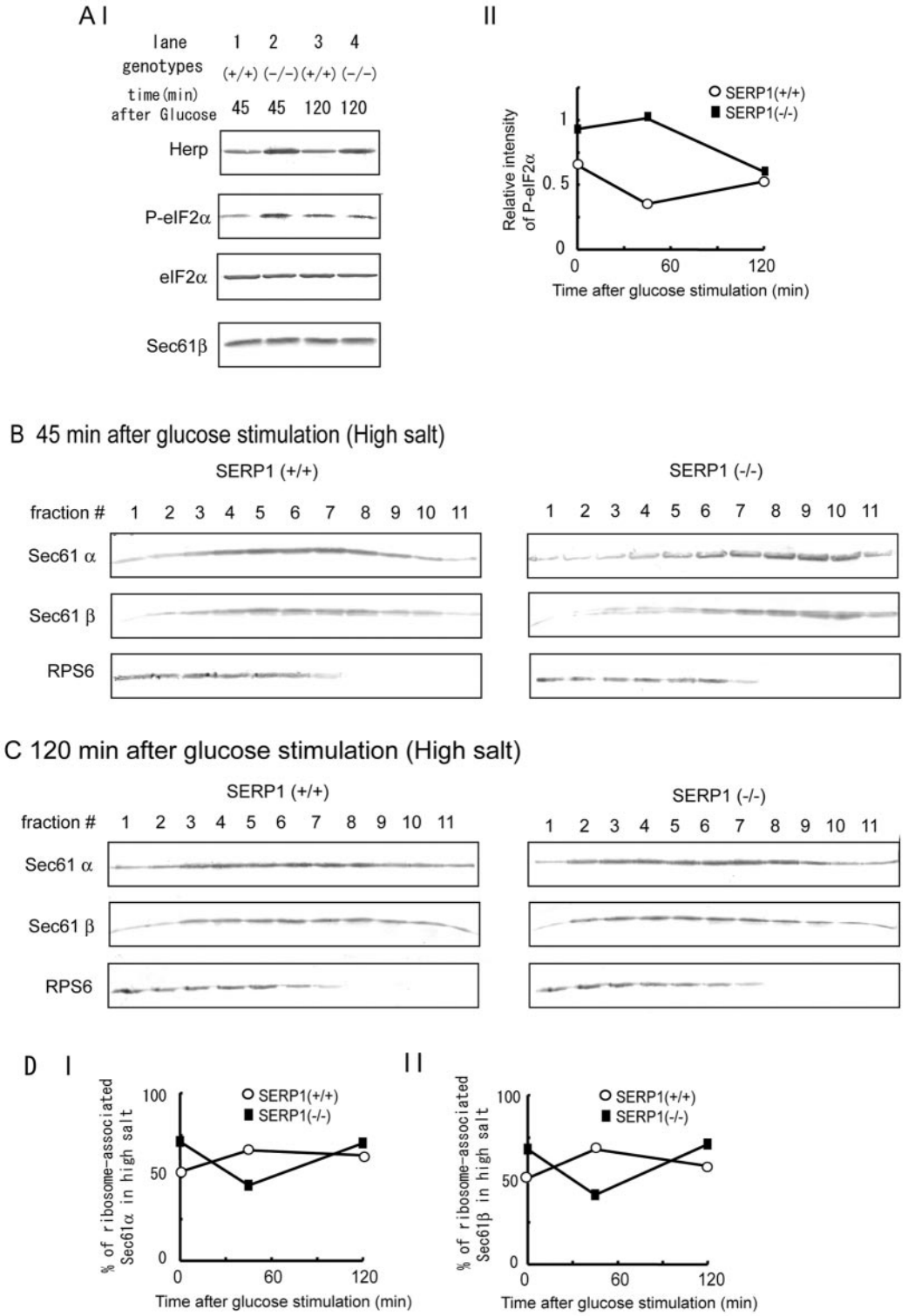

FIG. 7. Characterization of pancreatic RM after glucose stimulation. A. Expression of ER stress-related molecules and the Sec61 complex. I. RM were isolated from SERP1$^{+/+}$ and SERP1$^{-/-}$ pancreas either 45 min or 120 min after glucose injection and subjected to Western blotting (10 eq/sample) using the indicated antibodies. A typical result of three experiments with independently prepared RM is shown. II. Relative intensity of phosphorylated eIF2α antigen after glucose injection. Quantification of P-eIF2α and eIF2α intensities in Fig. 6AI and Fig. 7AI was performed as described in the text, and the relative intensity of P-eIF2α was obtained by dividing the P-eIF2α intensity by eIF2α intensity. B and C. Fractionation of RM. RM samples obtained 45 min (B) and 120 min (C) after glucose injection were fractionated using an iodixanol gradient (20 to 30%) in high-salt conditions and subjected to Western blotting with the indicated antibodies. A typical result of three experiments with independently prepared RM is shown. D. Quantification of Sec61α and -β intensities was performed in Fig. 6D and Fig. 7B and C, and the ratio of ribosome-associated proteins to total proteins is shown.

SERP1$^{-/-}$ mice became more evident. In SERP1$^{+/+}$ mice, levels of phosphorylated eIF2α decreased by 45 min after a glucose load (Fig. 7AI and AII), and at this approximate time, biosynthesis of insulin/proinsulin reached a peak (Fig. 4D, lane 2). Consistent with these data, the Sec61 complex in SERP1$^{+/+}$ mice became more tightly associated with ribosomes (Fig. 7B, DI, and DII), which continued up to 120 min after glucose stimulation. In SERP1$^{-/-}$ mice, however, eIF2α was still phosphorylated, and biosynthesis of insulin/proinsulin was limited to low levels 45 min after glucose load (Fig. 4D, lane 6). More than half of the Sec61 complex in SERP1$^{-/-}$ mice was not tightly associated with ribosome at this time (Fig. 7B, DI, and DII). The status of protein translation in SERP1$^{-/-}$ mice changed 120 min after glucose stimulation. Levels of phosphorylated eIF2α decreased (Fig. 7AI and AII), and biosynthesis of insulin/proinsulin increased (Fig. 4D, lane 8). Furthermore, the Sec61 complex in SERP1$^{-/-}$ mice became more tightly associated with ribosomes again (Fig. 7C, DI, and DII). These observations further support an idea of the close correlation of enhanced ER stress, prolonged suppression of protein translation, and delayed insulin/proinsulin biosynthesis in SERP1$^{-/-}$ RM. Recently, it was reported that p58/IPK, an ER stress-inducible molecule, inhibits phosphorylation of PERK and regulates the PERK-eIF2α pathway (21). In our system, however, expression of p58/IPK decreased 120 min after glucose stimulation (data not shown).

Biosynthesis of polypeptide hormones requires tight regulation to ensure a burst of mature protein production over a short period in response to challenge without induction of protein overload in the ER. In accordance with this concept, the PERK-eIF2α pathway has a critical role in polypeptide hormone biosynthesis. Deletion of the PERK gene or mutational inactivation of eIF2α caused progressive pancreatic cell death and led to severe growth retardation and diabetes mellitus (6, 15, 22). It is noteworthy that phenotypes in SERP1$^{-/-}$ mice were generally milder than were those in PERK$^{-/-}$ or eIF2α-inactivated mice. Although some of the phenotypes in SERP1$^{-/-}$ mice were associated with activation of eIF2α, the PERK-eIF2α pathway may still function as a strong protective tool in SERP1$^{-/-}$ mice. In future studies with SERP1$^{-/-}$ mice, the status of ER stress and protein biosynthesis in different situations where SERP1 is also highly expressed, including exocrine systems and more pathological conditions, should be clarified.

ACKNOWLEDGMENTS

We are grateful to Jun-ichi Miyazaki (Osaka University), Hiroshi Kiyama (Osaka City University), Michael G. Katze (University of Washington), and Victor L. J. Tybulewicz (MRC National Institute for Medical Research) for providing MIN6 cells, Adex1CA GFP, anti-p58/IPK antibody, and pPNT vector, respectively. We thank Masahide Asano (Kanazawa University) and David Ron (New York University) for their valuable suggestions. We also thank Fusae Ichinoda and Harumi Nishihama for their technical assistance.

This work was partly supported by a grant-in-aid for scientific research (15032315) from the Ministry of Education, Science, Technology, Sports and Culture of Japan (to O.H.) and by Deutsche Forschungsgemeinschaft KA 1444 and the Fonds der Chemischen Industrie (to E.H.).

REFERENCES

1. **Brewer, J. W., and J. A. Diehl.** 2000. PERK mediates cell-cycle exit during the mammalian unfolded protein response. Proc. Natl. Acad. Sci. USA **97:**12625–12630.
2. **Görlich, D., S. Prehn, E. Hartmann, K.-U. Kalies, and T. A. Rapoport.** 1992. A mammalian homolog of SEC61p and SECYp is associated with ribosomes and nascent polypeptides during translocation. Cell **71:**489–503.
3. **Görlich, D., and T. A. Rapoport.** 1993. Protein translocation into proteoliposomes reconstituted from purified components of the endoplasmic reticulum membrane. Cell **75:**615–630.
4. **Gotoh, M., T. Maki, T. Kiyoizumi, S. Satomi, and A. P. Monaco.** 1985. An improved method for isolation of mouse pancreatic islets. Transplantation **40:**437–438.
5. **Harding, H. P., Y. Zhang, and D. Ron.** 1999. Translation and protein folding are coupled by an endoplasmic reticulum resident kinase. Nature **397:**271–274.
6. **Harding, H. P., H. Zeng, Y. Zhang, R. Jungries, P. Chung, H. Plesken, D. D. Sabatini, and D. Ron.** 2001. Diabetes mellitus and exocrine pancreatic dysfunction in perk−/− mice reveals a role for translational control in secretory cell survival. Mol. Cell **7:**1153–1163.
7. **Hori, O., F. Ichinoda, A. Yamaguchi, T. Tamatani, M. Taniguchi, Y. Koyama, T. Katayama, M. Tohyama, D. M. Stern, K. Ozawa, Y. Kitao, and S. Ogawa.** 2004. Role of Herp in the endoplasmic reticulum stress response. Genes Cells **9:**457–469.
8. **Itoh, N., and H. Okamoto.** 1980. Translational control of proinsulin synthesis by glucose. Nature **283:**100–102.
9. **Kutay, U., E. Hartmann, and T. A. Rapoport.** 1993. A class of membrane proteins with a C-terminal anchor. Trends Cell Biol. **3:**72–75.
10. **Miyazaki, J., K. Araki, E. Yamato, H. Ikegami, T. Asano, Y. Shibasaki, Y. Oka, and K. Yamamura.** 1990. Establishment of a pancreatic β cell line that retains glucose inducible insulin secretion: special reference to expression of glucose transporter isoforms. Endocrinology **127:**126–132.
11. **Mori, K.** 2000. Tripartite management of unfolded proteins in the endoplasmic reticulum. Cell **101:**451–454.
12. **Nagamatsu, S., T. Watanabe, Y. Nakamichi, C. Yamamura, K. Tsuzuki, and S. Matsushima.** 1999. α-soluble N-ethylmaleimide-sensitive factor attachment protein is expressed in pancreatic β cells and functions in insulin but not γ-aminobutyric acid secretion. J. Biol. Chem. **274:**8053–8060.
13. **Oyamadori, S., and M. Mori.** 2004. Roles of CHOP/GADD153 in endoplasmic reticulum stress. Cell Death Differ. **11:**381–389.
14. **Sakaguchi, M., C. Ueguchi, K. Ito, and T. Omura.** 1991. Yeast gene which suppresses the defect in protein export of a secY mutant of E. coli. J. Biochem. **109:**799–802.
15. **Scheuner, D., B. Song, E. McEwen, C. Lie, R. Laybutt, P. Gillespie, T. Saunders, S. Bonner-Weir, and R. Kaufman.** 2001. Translational control is required for the unfolded protein response and in vivo glucose homeostasis. Mol. Cell **7:**1165–1176.
16. **Schroder, K., B. Martoglio, M. Hofmann, C. Holscher, E. Hartmann, S. Prehn, T. A. Rapoport, and B. Dobberstein.** 1999. Control of glycosylation of MHC class II-associated invariant chain by translocon-associated RAMP4. EMBO J. **18:**4804–4815.
17. **Walter, P., and G. Blobel.** 1983. Preparation of microsomal membranes for cotranslational protein translocation. Methods Enzymol. **96:**84–93.
18. **Webb, G. C., M. S. Akbar, C. Zhao, and D. F. Steiner.** 2000. Expression profiling of pancreatic β cells: glucose regulation of secretory and metabolic pathway genes. Proc. Natl. Acad. Sci. USA **97:**5773–5778.
19. **Welsh, M., N. Scherberg, R. Gilmore, and D. F. Steiner.** 1986. Translational control of insulin biosynthesis. Evidence for regulation of elongation, initiation and signal-recognition-particle-medicated translational arrest by glucose. Biochem. J. **235:**459–467.
20. **Yamaguchi, A., O. Hori, D. M. Stern, E. Hartmann, S. Ogawa, and M. Tohyama.** 1999. Stress-associated endoplasmic reticulum protein 1 (SERP1)/ribosome-associated membrane protein 4 (RAMP4) stabilizes membrane proteins during stress and facilitates subsequent glycosylation. J. Cell Biol. **147:**1195–1204.
21. **Yan, W., C. L. Frank, M. J. Korth, B. L. Sopher, I. Novoa, D. Ron, and M. G. Katze.** 2002. Control of PERK eIF2α kinase activity by the endoplasmic reticulum stress-induced molecular chaperone P58^{IPK} Proc. Natl. Acad. Sci. USA **99:**15920–15925.
22. **Zhang, P., B. McGrath, S. Li, A. Frank, F. Zambito, J. Reinert, M. Gannon, K. Ma, K. McNaughton, and D. R. Cavener.** 2002. The PERK eukaryotic initiation factor 2α kinase is required for the development of the skeletal system, postnatal growth, and the function and viability of the pancreas. Mol. Cell. Biol. **22:**3864–3874.